

# Daylighting performance of offices with controlled shades

Hui Shen, Athanasios Tzempelikos

**Abstract**—Energy conservation in buildings is critical in order to reduce energy consumption and greenhouse gas emissions. This paper presents a dynamic daylighting simulation model to evaluate the combined impact of façade design parameters on the overall daylighting performance of perimeter office spaces. Annual advanced daylighting metrics and lighting energy consumption are computed as a function of the following façade design parameters: window-to-wall ratio, glass transmittance, controlled shading transmittance and orientation, for three different locations in the United States. Initially the analysis is performed without shading, followed by automated operation of roller shades preventing direct sunlight to enter the space for each orientation in order to avoid glare. For all locations, daylight “saturation” is observed for window-to-wall ratios higher than 40%. The results show that for private offices, north and east facing facades allow higher daylight provision due to shading operation during working hours. Energy savings due to reduction in lighting energy using lighting controls demand are analytically presented for all studied cases.

**Keywords**—daylighting, buildings, energy conservation, simulation, control.

## I. INTRODUCTION

WINDOWS are the most critical components of commercial building facades. Their shape, size and optical properties determine indoor daylighting conditions and visual comfort [1], [2]. Optimized glass façade design may improve exploitation of daylight and result in significant savings in electricity consumption for lighting [2], [3]. On the other hand, computational models that consider comprehensive building simulation are needed for prediction of illuminance on the interior surfaces of a building as well as on the work plane level [4]. Although various calculation models are available [5]-[7], they usually have some limitations in room geometry inputs, sky luminance inputs or evaluation metrics [4], [8]. Moreover, it is complicated to modify existing codes to adapt specific necessities or present results using different measures. As to the latter, advanced daylighting metrics may be properly used in daylighting performance evaluation [9]-[10].

This paper presents a flexible daylighting simulation model

A. Tzempelikos is with the School of Civil Engineering, Purdue University, West Lafayette, IN 47907 USA. Tel.: 765-496-7586; Fax: 765-494-0395; email: ttzempel@purdue.edu.

H. Shen is with the School of Civil Engineering, Purdue University, West Lafayette, IN 47907 USA (shen34@purdue.edu).

for calculation of hourly illuminance values on any interior surface. The model uses a combined one-bounce ray-tracing and radiosity method for computation of illuminance values. Daylighting metrics such as daylight autonomy and useful daylight illuminances are computed as a function of façade parameters (window size, properties, orientation and geometry) for different climatic locations in the US. A simple shading control measure is also applied to investigate the impact of shading and potential energy savings with lighting controls.

## II. DAYLIGHTING SIMULATION MODEL

### A. Exterior and transmitted illuminance

Direct and diffuse illuminance from the sky and the ground are calculated separately using the Perez luminous efficacy model [11]. The input data of Perez model including hourly beam normal irradiance, beam and diffuse horizontal irradiance and dew-point temperature were obtained from TMY3 weather data [17]. The output of the model is hourly direct and diffuse illuminance on the façade. After calculation of direct and diffuse incident illuminance on the windows, the transmitted daylight is computed by multiplying the hourly values with the respective varying glass visible transmittance. Beam transmittance is input as a function of the solar incidence angle (Fig. 2), whereas diffuse transmittance is set equal to the beam transmittance for incidence angle equal to  $60^\circ$ .

### B. Work plane interior illuminance

The model calculates directly transmitted daylight and diffuse incoming light at each time step (hourly throughout the year). For direct transmission under the “no shading” case, a one-bounce ray-tracing method is used to track the exact projection of the window (beam illuminance) on the floor, which is then treated as an extra surface with initial luminous exitance in the radiosity calculations. For diffuse daylight, the window interior surface is considered as diffuse luminous source emitting daylight uniformly towards all directions. The calculation model treats the situation by identifying whether the window projection is on floor. If not, the window has an initial luminous exitance equal to the total transmitted illuminance, otherwise the window has an initial luminous exitance equal to the transmitted diffuse illuminance and the floor has the remaining part of transmitted direct illuminance. By making such an assumption, the room is modeled by eight

surfaces: the window, the non-lit part of floor, the ceiling, the two sidewalls, the wall containing the window, the back wall, and the window (sunlit) projection on floor. The window and its projection on the floor have variable luminous exitances depending on the solar position and sky conditions. When the simple shading control measure is applied, the window always has an initial luminous exitance equal to the total transmitted illuminance which may be further blocked by shading device.

The final luminous exitances of all interior surfaces after inter-reflections in the room are then calculated via radiosity method [12].

$$M = (I - T)^{-1} \cdot M_0 \quad (1)$$

where  $M_0$  is the initial (source) luminous exitance matrix,  $I$  is the  $8 \times 8$  identity matrix and  $T$  is a matrix whose elements are given by  $T_{ij} = \rho \cdot F_{ij}$ ,  $F_{ij}$  being the view factor from surface  $i$  to surface  $j$  and  $\rho$  being the surface reflectance.

The illuminance for representative points on the work plane can be calculated by:

$$E = \sum M_i \cdot C_i \quad (2)$$

where  $C_i$  is the configuration factor between the investigated point and interior surface  $i$ . Note that this entire calculation is done for each hour in the year for a pre-selected grid on the work plane surface.

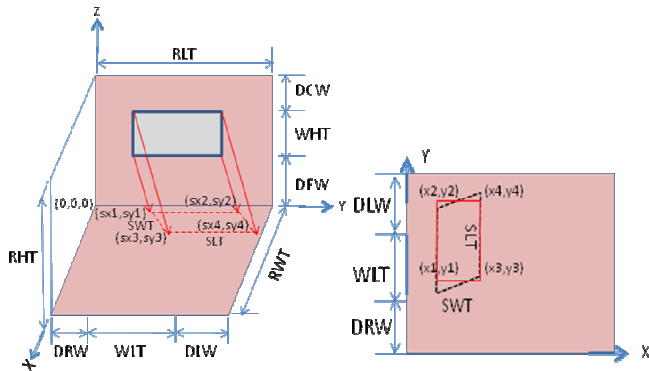


Fig. 1 Coordinate system and window projection on floor (left) and equivalent sunlit floor area using a rectangle approximation (right)

### C. Hourly calculation of variable view factors between all interior surfaces

The model calculates the window projection (sunlit area) on the floor. The shape, position and size of window projection vary with time in a day and day number, and hence the view factors between all interior surfaces change every hour. In order to calculate these varying view factors, the geometry shown in Fig. 1 was used in Cartesian coordinates. The origin is at the lower right corner of the wall containing the window.

Since it is complicated and time consuming to calculate the view factors between the window projection and other interior

surfaces using the actual shape of the sunlit area, the model transforms the shape of the sunlit area to an “equivalent” rectangle of equal area so that view factors can be computed faster without noticeable errors (Fig. 1). The hourly coordinates of the projected sunlit area on the floor can be calculated using the following equations:

$$\left[ \begin{array}{l} sx1_{n,t} = sx2_{n,t} = \frac{DFW}{\tan(\alpha_{n,t})} \cdot \cos(\gamma_{n,t}) \\ sx3_{n,t} = sx4_{n,t} = \frac{DFW + WHT}{\tan(\alpha_{n,t})} \cdot \cos(\gamma_{n,t}) \\ sy1_{n,t} = DRW - \frac{DFW}{\tan(\alpha_{n,t})} \cdot \sin(\gamma_{n,t}) \\ sy2_{n,t} = DRW + WLT - \frac{DFW}{\tan(\alpha_{n,t})} \cdot \sin(\gamma_{n,t}) \\ sy3_{n,t} = DRW - \frac{DFW + WHT}{\tan(\alpha_{n,t})} \cdot \sin(\gamma_{n,t}) \\ sy4_{n,t} = DRW + WLT - \frac{DFW + WHT}{\tan(\alpha_{n,t})} \cdot \sin(\gamma_{n,t}) \end{array} \right] \quad (3)$$

where  $n$  is day number,  $t$  is solar time,  $\alpha$  is solar altitude, and  $\gamma$  is the surface solar azimuth –distances are described in Fig. 1. The coordinates of the equivalent projected rectangular are given by:

$$\left[ \begin{array}{l} x1_{n,t} = x2_{n,t} = sx1_{n,t} \\ x3_{n,t} = x4_{n,t} = sx3_{n,t} \\ y1_{n,t} = y3_{n,t} = sy1_{n,t} + \frac{sy3_{n,t} - sy1_{n,t}}{2} \\ y2_{n,t} = y4_{n,t} = sy2_{n,t} + \frac{sy4_{n,t} - sy2_{n,t}}{2} \end{array} \right] \quad (4)$$

The hourly dynamic view factors throughout the year can then be obtained after determining the relative coordinates (Eq. (4)) of the sunlit floor area [13]. For faster computation, the area-weighted reflectance of the exterior (including the window) can be used.

## III. MODEL PARAMETERS AND STUDIED VARIABLES

### A. Building description and work plane illuminance grid

A typical office space with dimension of  $4 \times 4 \times 3$  m was considered. The reflectivities of the window, floor, ceiling and walls are set equal to 0.2, 0.3, 0.8 and 0.5 respectively. The window sill height is 0.8 m, same as work plane height. The work plane calculation grid consists of 9 points. One point merits mention is that all the dimensions can be changed easily in the calculation model to be applied to any building situation.

### B. Façade design variables

Several design variables were considered including building location, window size (expressed as window-to-wall ratio WWR), glass transmittance and orientation. More specifically, this paper includes results for:

- Three cities representing different climatic zones in the US are selected: Chicago, New York and Los Angeles;
- Four WWR values: 15%, 30%, 50% and 70% ;
- Three types of glass, with direct visible normal transmittance equal to: 80%, 60% and 40% respectively;
- All four main orientations (south, west, east and north).
- Three types of roller shades, with visible transmittance equal to: 3%, 5% and 7% respectively.

The variation of direct glazing transmittance with solar incidence angle is shown in Fig. 2.

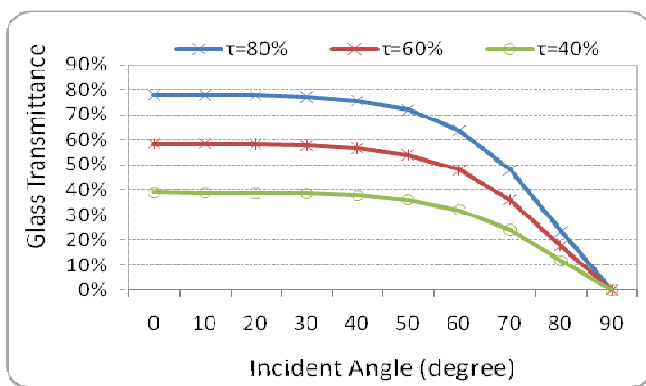


Fig. 2 Variation of beam glass transmittance with solar incidence angle

### C. Daylighting performance metrics

Hourly work plane illuminance values without shading are first calculated for the entire year. However, this is a “static” index that cannot be used to describe the overall annual daylighting performance of a specific design, since there are 8760 values for each calculation point. Daylight autonomy, an annual measure of how often a minimum work plane illuminance requirement of 500lx (typical set point) can be met by daylight alone, is calculated for the work plane grid for all working hours in the year (9am-5pm). This index includes the impact of all variables (climate, window size and properties, room geometry, etc) and can be also used to predict lighting energy savings if lighting controls are to be used [2]. A limitation of daylight autonomy is that it excludes illuminance values slightly below the threshold (that are useful) and that it does not consider the problem of glare due to excessive daylight. Hence, another metric called useful daylight illuminances is also calculated. It defines the illuminances that fall within the range of 100-2000lx as useful daylight illuminances [8]-[9]. In the present study, in order to systematically investigate the work plane illuminance profiles we subdivide the range of useful daylight illuminance into three bins: 100-500lx, 500-1000lx and 1000-2000lx. Two more parameters were computed that could be useful for future glare index estimation and for a subsequent thermal analysis:

- The minimum horizontal distance between the sunlit area (projected on the work plane) and the façade;
- The percentage of directly illuminated floor area.

### D. Shading control

Controlled shading devices can be adjusted to changing outdoor conditions based on different criteria, for example glare index values [14] and transmitted/incident beam radiation [15]. For office spaces, it is generally believed that direct sunlight is not allowed to enter the room in order to avoid glare and overheating problems. In this paper, roller shades with constant transmittance installed inside is considered. It would be close to allow diffuse light into the room when direct sunlight appears. It is controlled as following: when the incident irradiance on façade is over 130 W/m<sup>2</sup> the shade would close and otherwise open completely to allow diffuse light in the room.

## IV. RESULTS AND DISCUSSION

### A. “No shading” case

The calculated results are presented in comparative tables and graphs below. The impact of location, WWR, glazing transmittance and orientation were examined in detail. Table 1 shows the average annual daylight autonomy and useful daylight illuminance ratios (on work plane) for a south facing facade. Los Angeles has the highest daylight autonomy and useful daylight illuminance ratio. This is because Los Angeles locates at lower latitude and its climate is subject to a large amount of sunshine hours. In each location, daylight autonomy increases with the increase of window to wall ratio and glazing transmittance. However, useful daylight illuminance ratio presents more complex and interesting trends. Within UDI bin 1(100-500lx), UDI ratio decreases when window size and glazing transmittance increase. In UDI bin 2(500-1000lx), maximum UDI ratio appears at glazing transmittance equal to 60% for 15% window to wall ratio, and at 80% for other window size options. Also, the UDI ratio decreases with the increase of window size when transmittance is 80% or 60%, but maximizes at 30% window to wall ratio when the glazing

Location	New York			Los Angeles			τ
	WWR	80%	60%	40%	80%	60%	
DA (%)	15%	72.2	63.1	45	82.6	70.9	52.3
	30%	89.2	84	73.6	95.3	92.9	85.1
	50%	94.3	91.8	85.5	97.3	96.2	93.7
	70%	96	94.3	90.2	98	97.2	95.6
UDI (%) 100-500lx	15%	24.1	31.4	43.5	15.8	26.7	43.7
	30%	8.9	13.6	22.9	4.5	6.5	13.4
	50%	4.2	6.6	12.2	2.7	3.8	5.8
	70%	2.7	4.2	7.9	2	2.8	4.3
UDI (%) 500-1000lx	15%	24.6	26.8	24.9	30.3	30.9	27.6
	30%	15.5	19.1	25.2	10.1	19.1	31.2
	50%	8.8	12.9	18.5	3.6	6	16.4
	70%	5.7	9	14.8	2.4	3.5	8.3
UDI (%) 1000-2000lx	15%	24.9	21.6	14.9	27.6	24.4	16.7
	30%	25.2	29.1	26.9	31.2	33.6	30.7
	50%	18.5	22.9	29	16.4	27.6	35.5
	70%	14.8	19.1	25.2	8.3	16.7	32.2

transmittance is equal to 40%. In UDI bin 3(1000-2000lx), similar but more complex trends can be observed.

TABLE 1 DAYLIGHTING PARAMETRIC ANALYSIS RESULTS

Orientation is another important variable and greatly affects the daylight autonomy as shown in Figure 4, taking Chicago as an example. As expected, daylight autonomy is highest when the façade is facing south. For each orientation, the daylight autonomy increases with the increase of window-to-wall ratio and glazing transmittance. However, Fig. 3 shows that for such a typical private office, 40% window-to-wall ratio is enough to exploit daylight since there is no significant increase in daylight autonomy for larger window size. This result is consistent with those of similar studies for other climates [2].

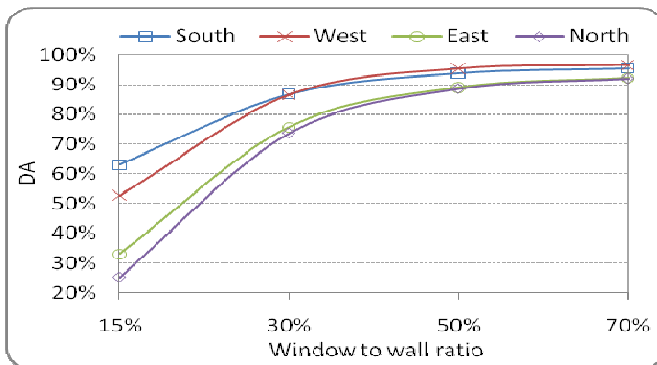


Fig. 3 Daylight autonomy as a function of window-to-wall ratio ( $\tau=60\%$ )

The authors believe that the amount of daylight falling in the range between 500lx and 1000lx is the most useful since it can offset electric lighting without causing glare; therefore, the useful daylight illuminance ratio is plotted as a function of window-to-wall ratio and glazing transmittance within UDI bin 2 for each orientation, (Fig. 4).

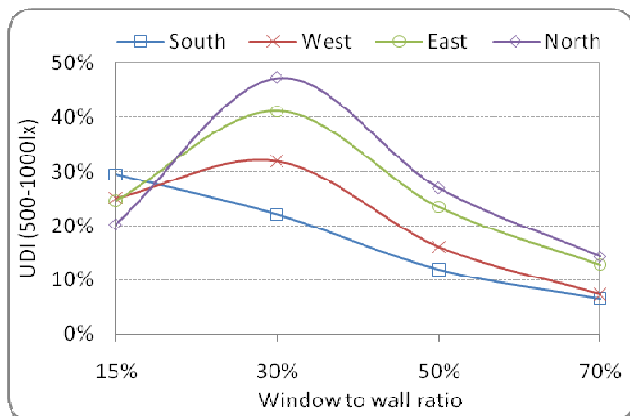


Fig. 4 Useful daylight illuminance ratio as a function of window-to-wall ratio ( $\tau=60\%$ )

With the increase of window size, UDI ratios show similar trends for all orientations except south—they first increase to maximum values at 30% window size and then decrease gradually to around 10-15%. As for south facing windows, the UDI ratio continually decreases with the increase of window size. This is explained by the fact that south windows receive

much more daylight than other orientations, so when window size increases, the average illuminance on work plane may increase to more than 1000lx and thus decreases the UDI ratio for this bin. As to the other three orientations, a larger window size also increases the average illuminance and excludes some hours just below the upper limit of 1000lx out of the daylight illuminance range. But increase of window size results in more hours when otherwise may be below the lower limit of 500lx into the daylight illuminance range. This explains why UDI ratios reach a maximum values around 30% WWR.

Glare is always a problem in perimeter spaces with windows [16]. In the absence of shading devices (which are essential) proper arrangement of work space positions is important to reduce visual discomfort. Areas that are frequently sunlit should be avoided. Fig. 5 shows the maximum and minimum horizontal distance between the sunlit area on floor and the facade during three representative days. For a given room, larger solar altitude or larger surface solar azimuth would result in smaller distances. In general, the sunlight enters into the deep part of a space due to lower solar altitude in winter. In the morning and afternoon, lower solar altitude may result in larger distance. But at those times, the surface solar azimuth is also high, which has adverse effect on the distance. As shown in Fig. 5, solar altitude plays a more important role in winter, so the minimum distance has two peaks at near 9am and 3pm. In summer, surface solar azimuth overwhelms solar altitude, so the maximum distance appears near noon.

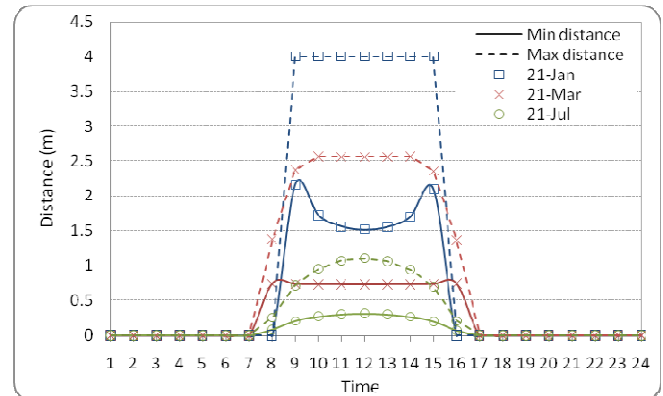


Fig. 5 Maximum and minimum horizontal distance between sunlit area and a south-facing façade in Chicago

The last calculated parameter, the fraction of sunlit area of the work plane surface is shown for every hour in the year in Fig. 6. Higher values are realized in winter because of low solar altitude angles. They maximize around noon, since for early morning and late afternoon the window projection is on the side walls instead of the work plane surface (or floor).

#### B. Controlled interior shades

Shading provision is essential in order to avoid glare and overheating. After implementing shading controls in the models, daylighting performance metrics significantly change for every location. Figs. 7-9 show the respective daylight autonomy results as a function of WWR, glazing and shading

transmittance for the three considered locations.

Los Angeles has more sunny skies than the other locations and therefore the shades have to automatically close more often in order to prevent glare. As a result, it has the lowest daylight autonomy. For all locations, the daylight autonomy naturally keeps increasing with the increase of window to wall ratio, shading transmittance and glazing transmittance. The results for useful daylight illuminance ratio show similar but even complex trends compared with the “no shading” case.

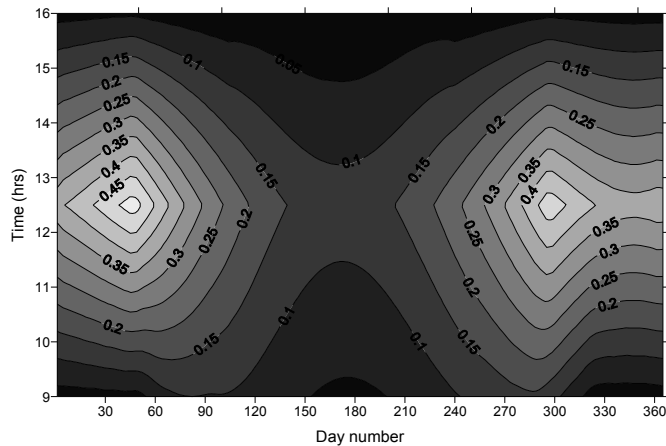


Fig. 6 Fraction of directly illuminated work plane area throughout the year (vertical axis= daily time) for a south-facing façade in Chicago

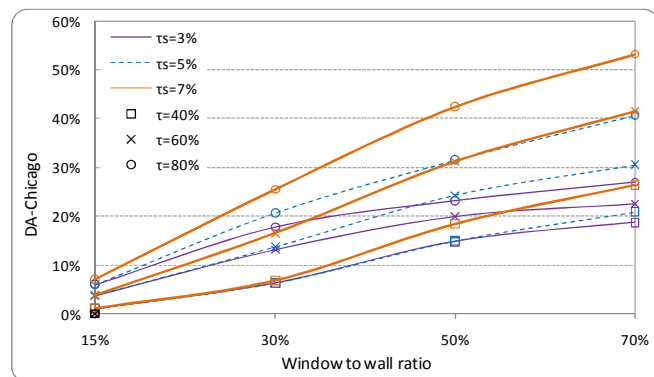


Fig. 7 Daylight autonomy as a function of WWR for three shading and three glazing types-Chicago

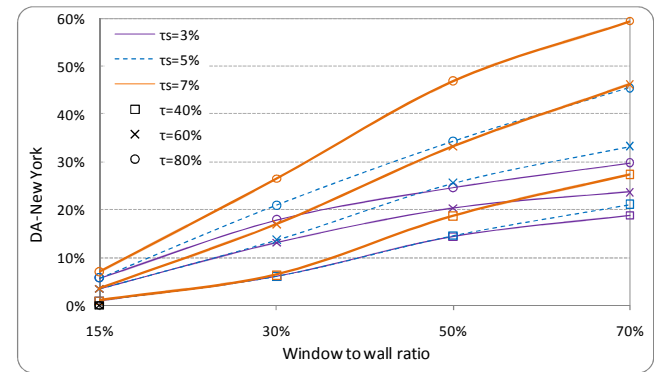


Fig. 8 Daylight autonomy as a function of WWR for three shading and three glazing types-New York

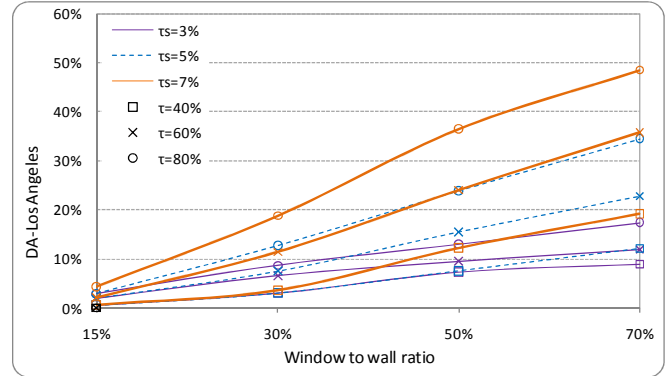


Fig. 9 Daylight autonomy as a function of WWR for three shading and three glazing types-Los Angeles

A controlled roller shade with 5% transmittance can provide an office space with 50% windows with all necessary daylight during 42% of the time in Chicago, 47% of the time in New York and 366% of the time in Los Angeles, assuming a clear glass with 80% transmittance. This indicates that lighting energy savings can be realized even with controlled shading.

Assuming on/off control of electric lights corresponding to available natural light levels, lighting energy savings can be calculated from the following equation [2]:

$$E_L = P_L \cdot A \cdot t_y \cdot DA \tag{5}$$

where  $P_L$  is the installed lighting power density ( $W/m^2$ ),  $A$  is work plane area ( $m^2$ ),  $t_y$  is the number of working hours in a year and  $DA$  is the annual average daylight autonomy. For the considered private office with  $16 m^2$  floor area and a lighting power density of  $11 W/m^2$  (typical value for energy efficient electric lighting installations), the predicted lighting energy savings are presented in Fig. 10 for Chicago as a function of shading transmittance and WWR when a clear glass is used (80% normal transmittance).

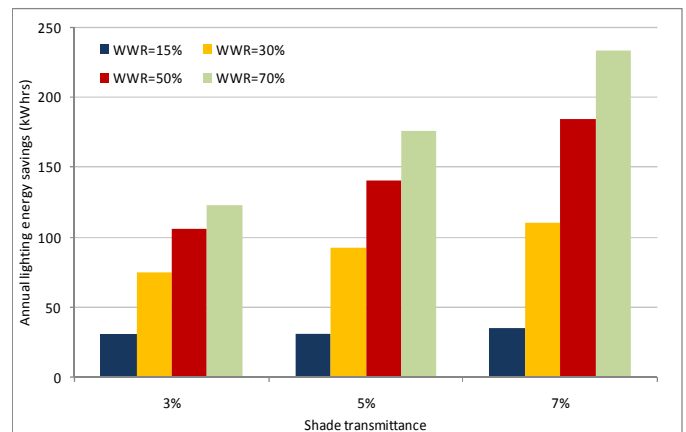


Fig. 10 Annual lighting energy savings with automated shading operation for a small private office in Chicago as a function of shade transmittance and WWR

## V. CONCLUSION

This paper presented a daylighting simulation model using hourly weather data and a combined radiosity/ray-tracing method for perimeter private offices. Using dynamic (variable) view factors, daylight performance metrics were computed as a function of façade parameters (window size, properties, orientation and geometry) in order to help the designers make better decisions related to optimal daylighting performance. Shading control was added in order to avoid glare and estimate annual energy savings from on/off lighting controls. This study is the basis for a future model that will include the impact of façade design variables for a complete evaluation of overall daylighting and thermal performance of office spaces.

## REFERENCES

- [1] C. Reinhart, "The annual daylight availability in peripheral offices in Canada – a simulation study". National Research Council of Canada, Report #44-B3213-L, 2002.
- [2] A. Tzempelikos, A. K. Athienitis, "The impact of shading design and control on building cooling and lighting demand", *Solar Energy*, vol. 81, pp. 369-382, 2007.
- [3] A. Tzempelikos, A. K. Athienitis, "Investigation of lighting, daylighting and shading design options for new Concordia University engineering building", in *Proc. of eSim2002*, Montreal, Canada, pp. 177-184, 2002.
- [4] A. Rosa, V. Ferraro, N. Igawa, D. Kaliakatsos, V. Marinelli, "INLUX: A calculation code for daylight illuminance predictions inside buildings and its experimental validation", *Building and Environment*, vol. 44, pp. 1769-1775, 2009.
- [5] W. L. Carrol, *Daylighting simulation: methods, algorithms, and resources*. Report of IEA SHC Task21/ECBCS ANNEX 29 and Lawrence Berkeley National Laboratory LBNL-44296, 1999.
- [6] J. Mardaljevic, "The BRE-IDMP dataset: a new benchmark for the validation of illuminance prediction techniques", *Lighting Research and Technology*, vol. 33, no 2, pp. 117-136, 2001.
- [7] G. Ward, R. Shakespeare, "Rendering with RADIANCE: the art and science of lighting visualization", Space and Light, California, USA, 2003.
- [8] A. Nabil, J. Mardaljevic, "Useful daylight illuminances: a replacement for daylight factors", *Energy and Buildings*, vol. 38, pp. 905-913, 2006.
- [9] A. Nabil, J. Mardaljevic, "Useful daylight illuminances: a new paradigm for assessing daylight in buildings", *Lighting Research and Technology*, vol. 37, no 1, pp. 41-57, 2005.
- [10] C. Reinhart, J. Mardaljevic, Z. Rogers, "Dynamic daylight performance metrics for sustainable building design", *LEUKOS*, vol. 3, no.1, pp. 1-25, 2006.
- [11] R. Perez, P. Ineichen, R. Seals, "Modeling daylight availability and irradiance components from direct and global irradiance", *Solar Energy*, vol. 44, no. 5, pp. 271-289, 1990.
- [12] C. Goral, K. Torrance, D. Greenberg, B. Battaile, "Modeling the interaction of light between diffuse surfaces", *Computer Graphics*, vol. 18, no. 13, pp. 213-222, 1984.
- [13] J. Murdoch, *Illuminating engineering: from Edison's lamp to the LED*. 2<sup>nd</sup> edition, Visions Communications, New York, USA, 2003.
- [14] E. Lee, S. E. Selkowitz, "The design and evaluation of integrated envelope and lighting control strategies for commercial buildings", *ASHRAE Transactions*, vol. 101, no. 1, pp. 326-342, 1995.
- [15] C. F. Reinhart, C. Jones, "Electric lighting energy savings for an on/off photocell control- a comparative simulation study using DOE 2.1 and DAYSIM", in *Proc. eSim2004*, Vancouver, Canada, 2004, pp. 183-189.
- [16] K. Kim, B.S. Kim, S. Park, "Analysis of design approaches to improve the comfort level of a small glazed-envelope building during summer", *Solar energy*, vol. 81, no. 1, pp. 39-51, 2007.
- [17] National Renewable Energy Laboratory, *National solar radiation data base typical meteorological year 3 database*, 2005.

**Athanasios Tzempelikos** (B.Sc. in Physics, University of Athens, Greece, 1999, M.A.Sc. in Building Engineering, Concordia University, Montreal, Canada, 2001, Ph.D. in Building Engineering, Concordia University, Montreal, Canada, 2005) is an Assistant Professor in the School of Civil Engineering and in the School of Mechanical Engineering (by courtesy) at Purdue University, West Lafayette IN, USA.

He was a Research Associate in the Canadian Solar Buildings Research Network (2005-2008) and a building energy consultant for several architectural and engineering firms in North America (2005-present). His research is focused on dynamic building facades, daylighting controls, thermal performance of buildings, building simulation and energy conservation in the built environment.

Dr. Tzempelikos is a Member of the Architectural Engineering Institute (AEI) of the American Society of Civil Engineers (ASCE), Associate Member of the American Society of Heating, Refrigerating and Air-Conditioning Engineers (ASHRAE), Member of the International Building Simulation Association, Member of the International Solar Energy Society, Advisory Member of the Commission Internationale de l'Éclairage in Canada, and has served as a Member of technical review panels for the United States Department of Energy, the United States Environmental Protection Agency and the United States Green Building Council.

**Hui Shen** (B. Eng. In HVAC Engineering, East China Jiaotong University, China, 2006, M.Eng. in HVAC Engineering, Tongji University, China, 2009) is a Ph.D. student in the School of Civil Engineering at Purdue University, West Lafayette IN, USA.